Am J Cancer Res 2026;16(2):402-417
www.ajcr.us /ISSN:2156-6976/ajcr0169854

Original Article

TREM2 inhibits cholangiocarcinoma progression by regulating the TGF-β/Smad2/3 signaling pathway

Xia Lei, Jinyong Hao, Yani Gou, Xiaojun Huang

Department of Gastroenterology, The Lanzhou University Second Hospital, Lanzhou, Gansu, China

Received November 7, 2025; Accepted January 23, 2026; Epub February 15, 2026; Published February 28, 2026

Abstract: Triggering receptor expressed on myeloid cells 2 (TREM2) is a transmembrane receptor involved in the initiation and progression of multiple cancers through various pathways. However, its role in cholangiocarcinoma (CCA) remains unclear. This study aimed to elucidate the expression characteristics and functions of TREM2 in cholangiocarcinoma (CCA). First, we assessed TREM2 expression in a retrospective cohort of 55 patients with CCA using immunohistochemistry (IHC) and confirmed its localization by double immunofluorescence staining. Second, functional assays were performed to evaluate effects of TREM2 on CCA cell proliferation, migration, and invasion. Finally, mechanistic studies focused on the TGF-β/Smad2/3 pathway and epithelial-mesenchymal transition (EMT), including drug-induced activation of the TGF-β signaling pathway. In vitro assessments evaluated gemcitabine sensitivity and apoptosis, while tumorigenicity was examined using a nude mouse xenograft model. The results demonstrated that TREM2 expression in both the tumor stroma and tumor cells was inversely correlated with clinicopathological aggressiveness: high TREM2 expression was associated with a lower T stage (P = 0.004) and a lower TNM stage (P = 0.026), whereas low TREM2 expression was an independent risk factor for poorer disease-free survival. Functional studies demonstrated that TREM2 overexpression inhibited cholangiocarcinoma cell proliferation, migration, and invasion, whereas TREM2 knockdown promoted these malignant phenotypes. Mechanistic investigations revealed that TREM2 reverses the expression of epithelial-mesenchymal transition (EMT) markers by inhibiting Smad2/3 phosphorylation, and these effects can be reversed by activators of the TGF-β signaling pathway. Additionally, TREM2 enhanced gemcitabine sensitivity by lowering the gemcitabine IC50 and promoting gemcitabine-induced apoptosis. Collectively, TREM2 exerts tumor-suppressive functions in cholangiocarcinoma and enhances chemotherapy sensitivity, suggesting its potential as a therapeutic target and prognostic biomarker.

Keywords: Cholangiocarcinoma, TREM2, clinicopathology, prognosis, EMT

Introduction

Cholangiocarcinoma (CCA), the second most common primary liver cancer after hepatocellular carcinoma, is a group of malignant tumors arising from the biliary tract [1]. CCA is classified based on its anatomical location into intrahepatic cholangiocarcinoma (iCCA) and extrahepatic cholangiocarcinoma (eCCA). eCCA is further differentiated into portal cholangiocarcinoma (pCCA) and distal cholangiocarcinoma (dCCA), depending on the cystic duct's confluence with the common bile duct [2]. The incidence of CCA rose by 43.8% (from 3.08 to 4.43 cases per 100,000 people per year) between 2001 and 2017, with incidence rates increasing with age, particularly among younger patients aged 18 to 44 years (81.0%) [3]. Due to the biliary system's unique anatomical location, early-stage lesions are difficult to detect through routine examinations. Consequently, most patients are diagnosed at an intermediate or late stage, leading to a surgical resection rate of approximately 20% to 30%. Palliative chemotherapy predominantly relies on gemcitabine-based regimens, which have limited efficacy; the overall 5-year survival rate is a mere 5% [4]. The high invasiveness of these tumors, coupled with their heterogeneity (both intra- and intertumoral) and resistance to chemotherapy, contribute to a poor prognosis and a high mortality rate for CCA patients [5]. Consequently, the identification of prognostic markers and potential therapeutic targets for CCA has become a critical research priority. Moreover, given the significant connective tissue hyperplasia characteris-

https://doi.org/10.62347/BYLB7175

tic of CCA, targeting the tumor immune microenvironment is likely to represent a promising therapeutic strategy.

The triggering receptor expressed on myeloid cells 2 (TREM2) is a transmembrane receptor belonging to the immunoglobulin superfamily, and it is primarily expressed on myeloid cells, notably cerebral microglia and peripheral macrophages [6]. It functions as a crucial immune signaling hub, modulating various pathological pathways. Initially studied in neurodegenerative diseases (NDDs), TREM2 was recognized as a critical regulator of microglial response and identified as a risk factor for Alzheimer's disease (AD) and other NDDs [7]. Over the past few years, as TREM2 has been found to be widely expressed on monocyte-macrophage lineage cells, increasing attention has been paid to its roles in the tumor microenvironment and cancer immunotherapy. Intriguingly, TREM2 is also widely expressed on tumor cells, where it can regulate proliferation and metastatic potential through multiple signaling pathways, thereby influencing tumor progression [8, 9]. For instance, TREM2 acts as an oncogene in gastric cancer (GC) [10] and esophageal adenocarcinoma (EAC) [11]. Conversely, it functions as a tumor suppressor in colorectal cancer (CRC) and hepatocellular carcinoma (HCC) by inhibiting critical pathways such as Wnt/β-catenin and PI3K/Akt [12-14].

Although the role of TREM2 in other malignant tumors has been confirmed, its expression pattern, functional significance, and potential mechanism in cholangiocarcinoma have not been investigated. Given the abundant extracellular matrix and immune infiltrates in CCA, together with evidence that TREM2 is involved in chemoresistance and epithelial-mesenchymal transition (EMT) in other cancers, we hypothesized that TREM2 plays a key regulatory role in CCA pathogenesis. To test this hypothesis, the design of this study is as follows: (1) Analyze the expression characteristics of TREM2 in clinical specimens of cholangiocarcinoma and correlate it with clinicopathological features; (2) Investigate the functional effects of TREM2 on the proliferation, migration, invasion and chemosensitivity of cholangiocarcinoma cells in vitro and in vivo; (3) Elucidate the molecular mechanism of TREM2 regulating TGF-β/Smad2/3 signaling pathway and epithelial-mesenchymal transition (EMT). Finally, this study aimed to reveal the multiple roles of TREM2 in the biology of cholangiocarcinoma and lay a foundation for its potential application as a prognostic marker and therapeutic target.

Materials and methods

Patients and tissue samples

This retrospective cohort study initially enrolled 68 patients who underwent surgical resection at Lanzhou University Second Hospital between 2021 and 2024 and had pathologically confirmed CCA. After screening based on inclusion and exclusion criteria, 55 cases were ultimately included for analysis. Inclusion criteria were: (1) histologically confirmed cholangiocarcinoma; (2) availability of paraffin-embedded tumor tissue suitable for immunohistochemical (IHC) testing; (3) complete clinical and pathological data (including T staging, AJCC staging, and recurrence follow-up information). Exclusion criteria were: (1) insufficient paraffin-embedded tumor tissue material or inability to perform IHC staining analysis; (2) incomplete clinical data or missing follow-up records (e.g., inability to obtain 1-year recurrence status). The collected clinicopathological information included gender, age, lesion location, degree of differentiation, tumor size, lymph node metastasis, TNM stage, preoperative serum bilirubin (TBIL), γ-glutamyl transferase (γ-GT), alkaline phosphatase (ALP), alpha-fetoprotein (AFP), carcinoembryonic antigen (CEA), carbohydrate antigen 125 (CA125), and carbohydrate antigen 199 (CA199) levels. The TNM staging of CCA was based on the AJCC 8th edition of the Cancer Staging Manual. None of the patients received chemotherapy, radiotherapy, or immunotherapy before surgery. Postoperative follow-up was 2 years. All patients provided written informed consent. The study protocol was approved by the Ethics Committee of the Second Hospital of Lanzhou University (Project number: 2023A-225).

Immunohistochemistry (IHC)

Paraffin-embedded tissue sections (4 μm) were prepared using a paraffin microtome (Leica RM2235, Germany). The sections were baked (Slide Mounting Machine, Leica, Germany, HI1220), dewaxed, and hydrated, and antigen retrieval was performed with sodium citrate buffer (10 mmol/L, pH 9.0). After washing in

PBS buffer, the sections were incubated with TREM2 primary antibody overnight at 4°C (1:100 dilution, ab318262, Abcam, Cambridge, UK). Subsequently, the samples were incubated with a horseradish peroxidase (HRP)-conjugated anti-rabbit IgG secondary antibody (1:500 dilution, Zen-bio, cat # 511203) for a duration of 30 minutes. Following incubation, the samples underwent repeated washing. The sections underwent incubation with diaminobenzidine solution and subsequent staining with hematoxylin. At least 3 points with the highest number of positive cells in each section were selected at 200× field of view using ImageJ software. Integrated optical density (IOD) and area were measured for each image to calculate the average optical density. The average optical density from three random areas per sample was then taken as the final value for that sample. Based on the mean %Area, samples were classified into three groups: high expression (≥4), medium expression (2-4), and low expression (0-2).

Immunofluorescence (IF)

Paraffin-embedded sections were deparaffinized and rehydrated, followed by antigen retrieval via microwave heating in EDTA buffer (pH 8.0). After blocking with BSA, the sections were stained with the antibodies. For tumor-cells localization, the sections were co-stained with TREM2 antibody (1:50 dilution, R&D Systems, cat # MAB17291) and CK19 antibody (Ready-to-use antibody, Maixin, cat # kit-0030) overnight at 4°C. For macrophage localization, sections were co-stained with TREM2 antibody (1:50 dilution, R&D Systems, cat # MAB17291) and CD68 antibody (Ready-to-use antibody, Maixin, cat # Kit-0026) overnight at 4°C. The sections were then incubated with the secondary antibody (Proteintech, cat # SA00003-11) was incubated at room temperature. Nuclei were counterstained with DAPI, autofluorescence was quenched using an autofluorescence quencher, and slides were mounted. The fluorescence microscope (Olympus BX53 + DP74) was used for microscopic examination.

Cell lines and cell culture

CCA cell lines (Hucct1, RBE, HCCC-9810) were purchased from Seville Biotechnology Co., Ltd. (Wuhan, China). The CCA cell line (SNU-1196) was purchased from Shanghai Central Asia Biotechnology Co., Ltd. (Shanghai, China). The normal cell line (Hibepic) was purchased from Huatuo Biotechnology Co., Ltd. (Shenzhen, China). All cell lines were authenticated by short tandem repeat (STR) profiling and used within 6 months of resuscitation. The cells were cultured in RPMI 1640 medium supplemented with 10% fetal bovine serum (FBS), 100 mg/mL streptomycin, and 100 U/mL penicillin. Cells were maintained at 37°C in a humidified incubator with 5% CO_2 (CO_2 Incubator, Heal Force, HF90).

Lentiviral transfection and screening

The well-conditioned target cells were digested and collected, inoculated into a 6-well plate at a density of 1×10^5 cells/mL, and 1 mL of medium was added to each well. After mixing, they were cultured in a 5% CO_2 incubator at 37°C. After 24 hours, the original medium was removed, and 1 ml of virus diluent (MOI = 20) and Polybrene (8 μg/mL) were added to each well. The cells were cultured in 5% CO_2 incubator at 37°C for 4 hours. After 4 hours, the experimental group was supplemented with 1 mL fresh complete culture medium and further cultured. On the second day after transfection, the culture medium containing the virus was removed, and fresh complete culture medium was added, and cells were further cultured. The fluorescence intensity was detected by inverted fluorescence microscope (Olympus IX53) 48 hours after transfection to assess transduction efficiency. Successfully transfected cells were screened by adding puromycin (3 μg/mL).

Cell proliferation assay

A Cell counting kit-8 (CCK-8) assay was used to analyze cell proliferation. Cholangiocarcinoma cells from different groups were harvested, counted, and plated into 96-well plates at 4×10^3 cells/well. Cells were incubated at 37°C in a humidified incubator with 5% CO_2 for 24, 48, 72, and 96 hours. Following incubation, 10 μL of CCK-8 solution was added to each well for 2 hours. The absorbance at OD_{450} in each well was measured using a BioTek full-wavelength microplate reader (BioTek, Synergy H1).

Wound healing assay

Cells were inoculated into 6-well plates at a density of 5-7 × 10^5 cells/mL. The following

day, when the cells reached approximately 90% confluence, vertical scratches were introduced into the confluent monolayer using the tip of a sterile 200 μL pipette. After washing once with PBS. Cells were then cultured in serum-free medium, and images were captured at 0 and 24 h using an inverted microscope (Olympus IX53).

Transwell invasion/migration assay

Hucct1 cells (4×10^4 cells) and RBE cells (5×10^4 cells) were resuspended in 100 μL serum-free medium and seeded into the upper chamber of Transwell inserts (8-μm pores, pre-coated with Matrigel for invasion assays). Then, 500 μL of complete medium supplemented with 20% fetal bovine serum (FBS) was added to the lower chamber as a chemoattractant and incubated for 24 h. Cells were fixed with paraformaldehyde for 30 min, stained with crystal violet for 30 min, and counted in five randomly selected fields (10×).

Terminal deoxynucleotidyl transferase dUTP nick end labeling (TUNEL) assay

The TUNEL assay was performed according to the manufacturer's instructions, the TUNEL assay was performed using the TUNEL Assay Kit (E-CK-A322, Elabscience). Briefly, cell slides were fixed with 4% paraformaldehyde, then incubated with the detection solution in the dark at 37°C for 60 minutes, followed by image acquisition with a fluorescence microscope (Olympus IX53).

Western blot analysis

Tissue samples and cell samples were collected, and total proteins were extracted using RIPA lysis buffer, PMSF, and phosphatase inhibitors. After protein standardization, tissue and cell samples were separated in SDS-PAGE (SDS-PAGE Protein Electrophoresis System, Bio-Rad, USA) and transferred to nitrocellulose membranes. The imprinting was then incubated with the corresponding primary and secondary antibodies and blocked with 5% skim milk. Signals were detected using an enhanced chemiluminescence (ECL, biosharp, cat # BL523A) substrate and imaged with a chemiluminescence imaging system (Fully Automated Chemiluminescence Image Processing System, Tanon, 5200 Multi). The list of antibodies is as follows: Phospho-Smad2 (1:1000 dilution, Cell Signaling Technology, cat # 8828), Phospho-Smad3 (1:1000 dilution, Cell Signaling Technology, cat # 9520), Smad3 (1:1000 dilution, HUABIO, cat # ET1607-41), Smad2 (1:5000 dilution, HUABIO, cat # ET1604-22), E-cadherin (1:2000 dilution, Proteintech, cat # 60335-1-Ig), N-cadherin (1:5000 dilution, Proteintech, cat # 66219-1-Ig), Vimentin (1:20000 dilution, Proteintech, cat # 60330-1-Ig), Slug (1:500 dilution, Proteintech, cat # 12129-1-AP), TREM2 (1:500 dilution, Proteintech, cat # 27599-1-AP), GAPDH (1:10000 dilution, Zen-bio, cat # 380626), and β-Tubulin (1:5000 dilution, Proteintech, cat # 80713-1-RR). Horseradish peroxidase (HRP)-conjugated anti-mouse IgG (1:10000 dilution, Zen-bio, cat # 511103) and anti-rabbit IgG (1:10000 dilution, Zen-bio, cat # 511203) were used as secondary antibodies for Western blotting. Quantitative analysis of protein expression was performed using ImageJ software.

Tumor formation model in nude mice

Twelve BALB/c nude mice were purchased from Changzhou Cavens Experimental Animal Co., Ltd. Four-week-old female nude mice were divided into two groups and subcutaneously injected with 1×10^6 cells (100 μL volume) of either Hucct1-OE-TREM2 or Hucct1-OENC cells, respectively. During the experiment, all animals were housed in a barrier environment at the Lanzhou Veterinary Research Institute of the Chinese Academy of Agricultural Sciences. Temperature was maintained at 22-25°C, with relative humidity controlled at 40-50%. Experimental animals were provided with autoclave-sterilized rodent complete nutrition feed and triple-purified drinking water. All procedures adhered to AAALAC International accreditation standards. Tumor size was monitored every three days, and tumor volume was calculated using the formula $V = ab^2/2$, where 'a' is the longest diameter and 'b' is the shortest diameter. Time-tumor volume growth curves were generated. Upon reaching a maximum tumor diameter of approximately 17 mm, the nude mice were euthanized by cervical dislocation. The subcutaneous tumor masses were then excised using a scalpel, and their volume, weight, and appearance were recorded, with representative images taken.

Statistical analysis

Statistical analysis was performed using SPSS Statistics 26.0, GraphPad Prism 10.0, and

ImageJ software for quantitative analysis. Continuous variables were expressed as mean ± standard deviation (SD) for normally distributed data and as median (interquartile range, IQR) for non-normally distributed data; categorical variables were expressed as counts (percentages). Normality was assessed using the Shapiro-Wilk test, and homogeneity of variance was evaluated using the Levene's test. Normally distributed data were analyzed using the unpaired Student's t-test; otherwise, the Mann-Whitney U test was applied. For comparisons involving three or more groups (e.g., low/medium/high TREM2 infiltration), data were analyzed using one-way ANOVA followed by an appropriate post hoc multiple-comparison test (Tukey's test for equal variances or Games-Howell test for unequal variances). For experiments involving two factors (e.g., genotype × drug treatment), two-way ANOVA was used with multiple comparison correction (e.g., Sidak or Bonferroni correction). For continuous data at multiple time points (such as the CCK-8 growth curve, tumor growth curves), we used repeated measures analysis of variance (RM-ANOVA). When dealing with two factors (group × time), two-factor repeated measures analysis of variance was applied, followed by post hoc multiple comparison corrections (Sidak method or Bonferroni method). The association between TREM2 expression and clinical-pathological factors was evaluated using chi-square tests or Fisher's exact tests. Factors with significant prognostic value were identified in univariate logistic regression analysis, and statistically significant (or clinically relevant) variables were subsequently incorporated into multivariate logistic regression models. Results were presented as odds ratios (OR) with 95% confidence intervals (CI). Disease-free survival (DFS) was analyzed using the Kaplan-Meier method, with intergroup differences compared via the log-rank test. Where applicable, the Cox proportional hazards model was used to estimate hazard ratios (HR) and their 95% confidence intervals. $P < 0.05$ was considered statistically significant.

Results

Association between the infiltration of TREM2-positive cells in the tumor stroma and clinicopathological parameters in CCA

A total of 55 retrospective cases were analyzed in this study (basic clinicopathological features of CCA patients are shown in Table S1), and TREM2 protein expression was assessed by immunohistochemistry. This study found that TREM2 was mainly expressed in immune cells within the tumor stroma as well as in tumor cells (**Figure 1A-C**). Furthermore, the level of TREM2 infiltration correlated with clinicopathological parameters. Therefore, according to the infiltration level of TREM2 positive cells (immune cells within the tumor stroma and tumor cells), cases were classified into three groups: low expression, medium expression and high expression. Associations were evaluated using the chi-square test, showing significant correlations between TREM2 expression and T stage ($P = 0.004$), AJCC stage ($P = 0.026$), and time to recurrence ($P < 0.001$). In patients with T1 stage, 0 cases were low expression, 6 cases (60%) were medium expression, and 4 cases (40%) were high expression. By contrast, in T4 patients, 12 cases (85.7%) were low expression, 2 cases (14.3%) were medium expression, and 0 cases were high expression. In addition, compared to the high TREM2 expression group, patients with low TREM2 expression showed a significantly higher proportion of Stage III (64.0%) and Stage IV (75%) disease, with no observed cases of Stage I (0%). Furthermore, patients with low TREM2 expression had a shorter time to recurrence, and 22 patients (66.7%) had disease progression, recurrence and metastasis within 1 year. Among patients with high TREM2 expression, 5 patients (71.4%) experienced no disease progression within 2 years, and 7 patients (46.7%) did not have tumor recurrence or metastasis within 1 year (Table S1).

The relationship between the infiltration level of TREM2 positive cells in tumor stroma and the disease progression of CCA patients

Univariate logistic regression analysis revealed that there was a significant correlation between the patients' tumor recurrence status at 1 year and TREM2 expression level ($P < 0.001$), T-stage ($P = 0.002$), AJCC stage ($P = 0.005$), and CEA level ($P = 0.017$) (Table S2). Subsequently, we included TREM2 expression level, AJCC stage, and CEA in a multivariate logistic regression analysis. In multivariable analysis, TREM2 expression level remained independently associated with recurrence ($P = 0.001$). Patients with low TREM2 expression had a high tumor recurrence rate within 1 year.

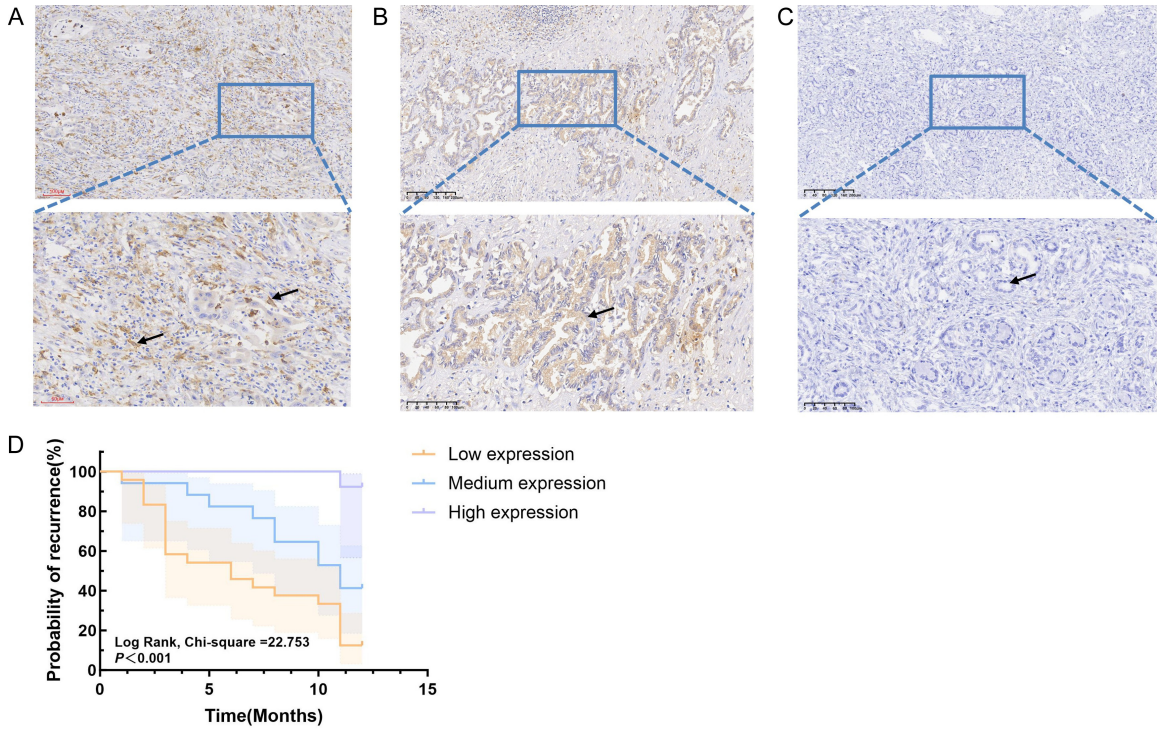

Figure 1. Immunohistochemical staining analysis of TREM2 expression levels in CCA tissue. A. TREM2 positive expression in immune cells within the tumor stroma, the black arrow indicates representative TAMs in the image (With magnification of 10× and 20×); B. After optimizing the immunohistochemical staining conditions, the results showed that TREM2 was also positively expressed in tumor cells, the black arrow indicates a representative tumor cell in the image (With magnification of 10× and 20×); C. Normal tissue with absent TREM2 expression, the black arrow indicates a representative normal cholangiocyte in the image (With magnification of 10× and 20×); D. Kaplan-Meier analysis of disease-free survival in patients with CCA based on TREM2 expression levels. Patients with CCA with low TREM2 expression had shorter disease-free survival than those with moderate and high expression ($P < 0.001$).

In order to further assess the relationship between tumor recurrence time and TREM2 expression in CCA patients, we used Kaplan-Meier analysis to evaluate the correlation between TREM2 expression levels and disease progression in CCA patients (**Figure 1D**). The results showed that the infiltration level of TREM2 positive cells in tumor stroma and tumor cells was related to the prognosis of disease progression, and high infiltration of TREM2 was a favorable prognostic factor for disease progression ($P < 0.001$).

Positive expression of TREM2 in tumor cells of patients with cholangiocarcinoma

IHC results showed that TREM2 was mainly expressed in immune cells within the tumor stroma as well as in tumor cells. In order to further clarify the expression of TREM2 in the tissues of cholangiocarcinoma, we used double immunofluorescence to co-localize CK19 (characteristic marker of cholangiocytes/cholangiocarcinoma) and TREM2. As shown in **Figure 2A**, the results showed that TREM2 was also positively expressed on tumor cells. Additionally, we used CD68 to label macrophages and found that TREM2 was also positively expressed on tumor-associated macrophages (**Figure 2B**).

Differential expression of TREM2 in Hibepic and CCA cell lines

The expression of TREM2 protein in Hibepic and Hucct1, RBE, HCCC-9810, SNU-1196 cells was detected by Western blotting (WB). TREM2 protein expression was higher in RBE, HCCC-9810 cell lines than in Hibepic ($P < 0.05$). Among the four CCA cell lines (Hucct1, RBE, HCCC-9810, and SNU-1196), the highest expression of TREM2 protein was found in HCCC-9810 cells, followed by RBE cells. Hucct1

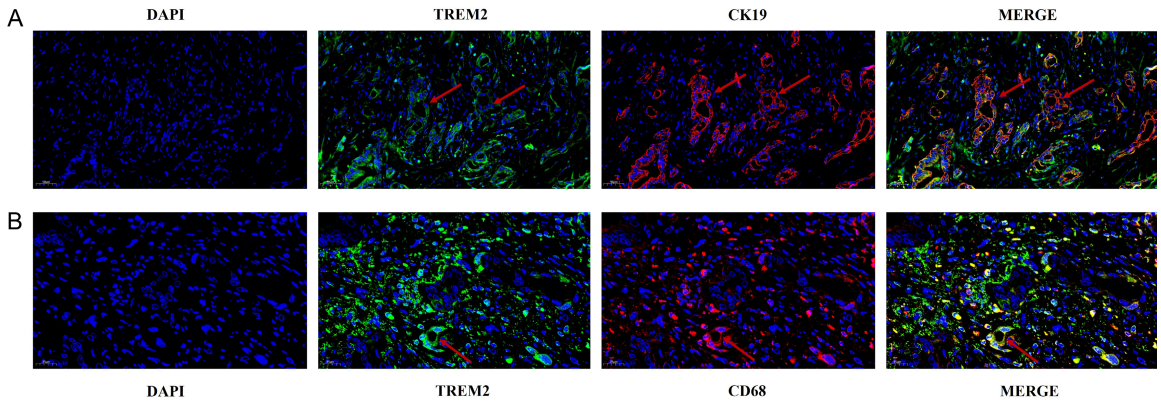

Figure 2. Double immunofluorescence staining localized TREM2 in the tissues of CCA patients. A. Co-staining of CCA patient tissue using TREM2 antibody and CK19 antibody: DAPI nuclear staining (blue); TREM2 immunofluorescence staining (green); CK19 immunofluorescence staining (red); Merged image showing co-localization of TREM2, CK19, and DAPI (With magnification of 20×); The red arrow refers to the representative tumor cells; B. Co-staining of CCA patient tissue using TREM2 antibody and CD68 antibody: DAPI nuclear staining (blue); TREM2 immunofluorescence staining (green); CD68 immunofluorescence staining (red); Merged image showing co-localization of TREM2, CD68, and DAPI (With magnification of 40×); The red arrow refers to the representative macrophages.

and SNU-1196 cells conversely showed the lowest TREM2 expression levels (Figure S1A). Therefore, we chose to upregulate TREM2 expression by lentiviral infection on Hucct1 (Figure S1C) and RBE cells (Figure S1D). WB results showed that the Hucct1-TREM2 overexpression group and the RBE-TREM2 overexpression group were significantly upregulated compared with the Vector group (Figure S1B). TREM2 expression was downregulated in RBE cells using CRISPR RNP, and WB results showed that the knockdown (KD) group was significantly downregulated compared to the wild type (WT) group.

TREM2 inhibits the proliferation, migration and invasion of CCA cells

To assess the biological functions of TREM2 in CCA cells, we employed CCK-8 and colony formation assays to evaluate proliferation capacity, and Transwell migration/invasion assays and wound healing assay to assess migration and invasion capabilities. The change of cell survival rate with time was analyzed by two-way repeated measures analysis of variance and Sidak's multiple comparison test. Our findings revealed that upregulating TREM2 in both Hucct1 and RBE cells significantly inhibited cell proliferation, migration, and invasion. Conversely, downregulating TREM2 expression in RBE cells promoted these malignant behaviors (**Figure 3**).

TREM2 inhibits EMT by inhibiting TGF-β/Smad signaling pathway

Based on the results of differential expression analysis, by setting the threshold |log2FC| > 1 and $P < 0.05$, a total of 1377 differentially expressed genes (DEGs) were identified, including 533 up-regulated genes and 844 down-regulated genes (**Figure 4A**). The volcano plot shows the directional changes of multiple molecules related to extracellular matrix/adhesion/epithelial-mesenchymal transition (such as the decreased expression of THBS1, FN1 and CDH2 in the OE group, while DCN increased), indicating that TREM2 may be involved in regulating the transcriptional programs related to the migration and invasion of cholangiocarcinoma cells. This finding is consistent with our previous experimental results. Further hierarchical clustering analysis was conducted on the differentially expressed genes (DEGs). The heat map of the differential genes showed that the samples within each group exhibited high clustering, while the samples from different groups were clearly separated (**Figure 4B**). This indicates that the repeatability within the sample groups is good, and the differences between the groups are stable and reliable. Functional enrichment analysis in GO analysis produced 368 significant items ($P < 0.05$), mainly involving processes related to epithelial-mesenchymal transition and migration (such as the positive regulation

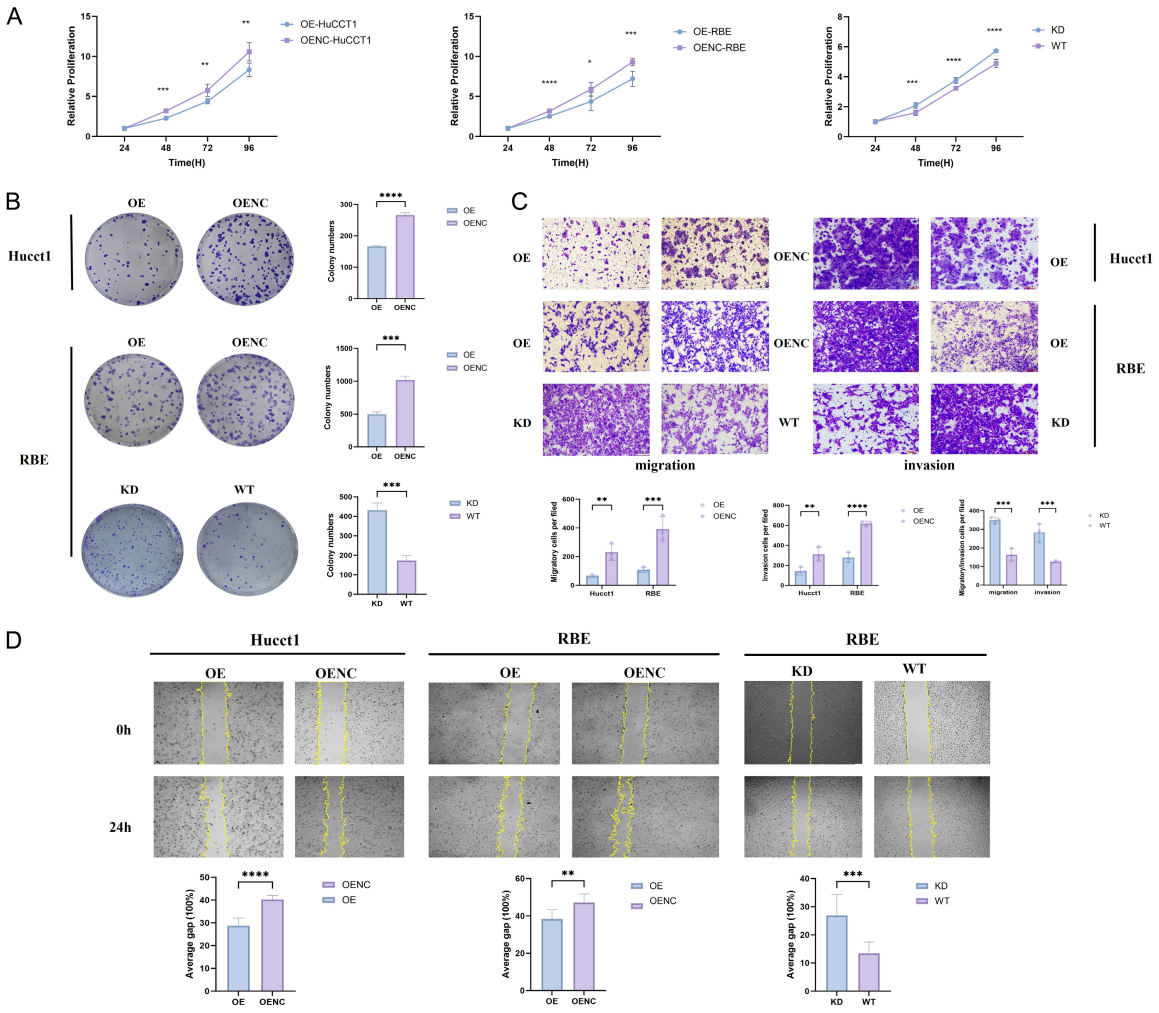

Figure 3. Effects of upregulating/downregulating TREM2 gene expression levels on the biological functions of CCA cells. A. The CCK-8 assay confirmed that upregulation/downregulation of TREM2 gene expression in Hucct1 and RBE cells inhibited/promoted the proliferation of CCA cells. B. Plate clone formation assays. C. Transwell migration/invasion assay (With magnification of 10×). D. cell wound healing assay (With magnification of 4×). OE group: Experimental group overexpressing the TREM2 gene; OENC group: Control group overexpressing a gene unrelated to the research subject or an empty vector; KD Group: Knockdown of TREM2 gene expression; WT group: Wild-type cell group.

of epithelial-to-mesenchymal transition, mesenchymal cell migration), immune receptor signal activation, and cell growth (**Figure 4C**). Further KEGG-GSEA analysis revealed 65 significantly enriched pathways ($P < 0.05$), among which 19 showed positive enrichment in the OE group and 46 showed negative enrichment in the control group. Notably, the TGF-β signaling pathway exhibited significant negative enrichment in the control group (NES = -1.564, P = 0.00711) (**Figure 4D**) and was downregulated in tandem with "ECM/adhesion/cytoskeletal remodeling" modules including ECM-receptor interaction, focal adhesion, and regulation of actin cytoskeleton (**Figure 4E**). The enrichment curve for the TGF-β signaling pathway further validated its significant negative enrichment under OE-TREM2 conditions (P = 0.00711) (**Figure 4F**). This suggests that TREM2 overexpression may suppress EMT-related molecular events and inhibit cholangiocarcinoma cell progression by inhibiting TGF-β signaling activity and concurrently reducing ECM/adhesion and cytoskeletal remodeling programs.

According to the above transcriptomic research results, TREM2 seems to have the ability to inhibit epithelial-mesenchymal transition (EMT)

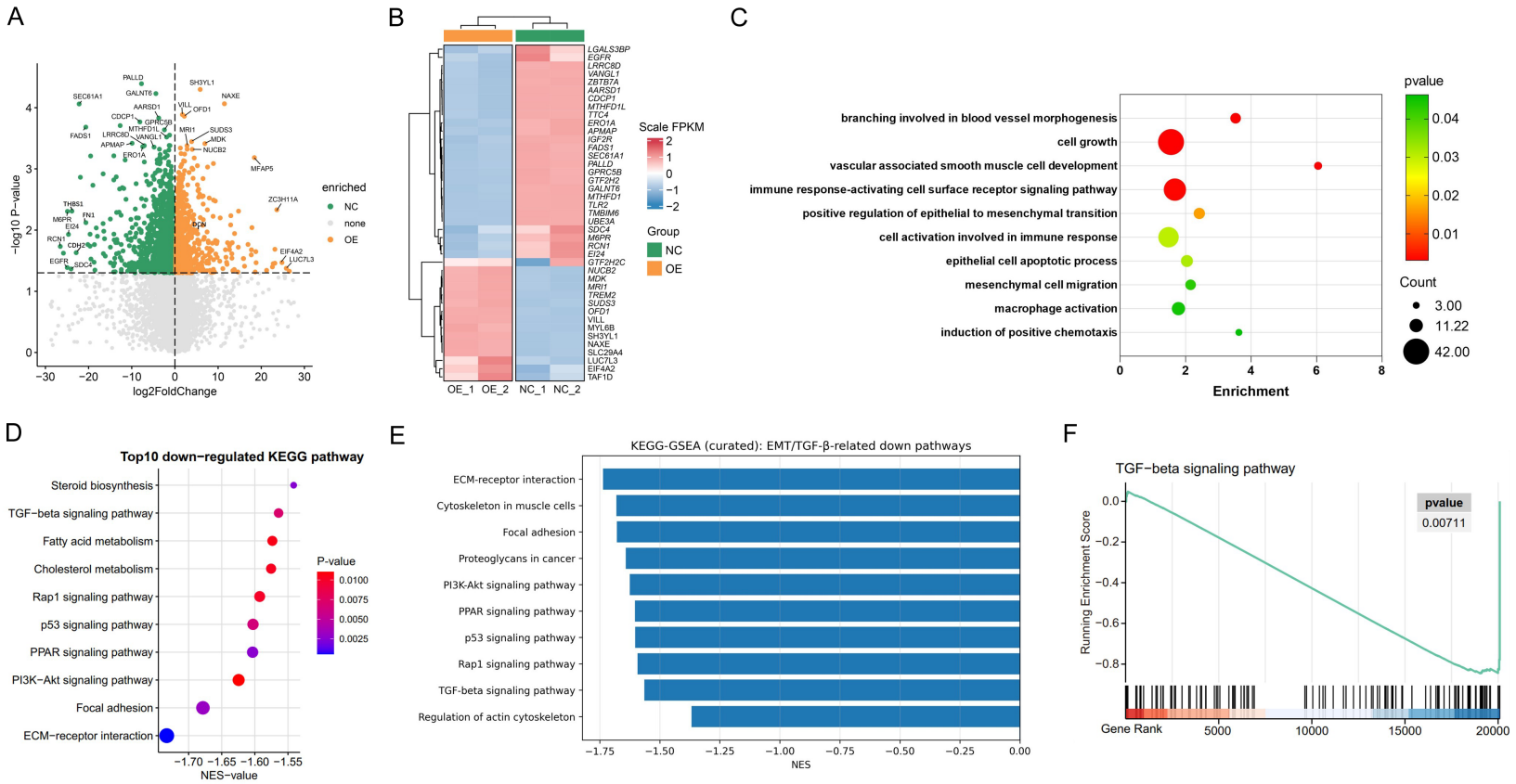

Figure 4. Transcriptomics differential expression and pathway enrichment analysis results. A. Volcano plot of differentially expressed genes, with log2FoldChange on the x-axis and -log10 (*P*-value) on the y-axis; dashed lines indicate threshold reference lines (P = 0.05 and |log2FC| > 1); B. Hierarchical clustering heatmap, with genes on the y-axis and standardized expression levels (Scale FPKM) represented by color; red indicates relatively high expression, blue indicates relatively low expression; C. GO Enrichment Analysis of Differentially Expressed Genes (Representative Entries) Bubble Chart: Vertical axis represents significantly enriched GO entry names; horizontal axis represents enrichment level (Enrichment); bubble size indicates number of enriched genes (Count); color indicates significance level (*P*-value); D. KEGG-GSEA Negative Enrichment Pathways Top 10 Displaying representative downregulated pathways with negative enrichment (NES < 0). The x-axis represents NES, and colors indicate *P*-values; E. Integrated visualization of EMT/TGF-β-associated downregulated pathways: A bar chart integrating pathways closely associated with EMT/TGF-β downregulation is presented. The horizontal axis represents NES (negative values indicate negative enrichment/downregulated enrichment), while the vertical axis displays pathway names; F. TGF-β signaling pathway GSEA enrichment curve: The upper curve represents the Running Enrichment Score, while the lower black vertical line indicates the distribution position of genes in this pathway within the full gene ranking.

and extracellular matrix (ECM) remodeling, which may be achieved by regulating the TGF-β signaling pathway. To further explore this mechanism, we conducted Western blot analysis to detect the protein levels of phosphorylated Smad2/3 and key EMT markers. As shown in **Figure 5**, compared with the control group, overexpression of TREM2 in Hucct1 and RBE cells led to a decrease in the phosphorylation levels of Smad2 and Smad3. At the same time, the expression of the epithelial marker E-cadherin increased, while the expressions of N-cadherin, vimentin, and Slug mesenchymal markers decreased. The total protein expression of Smad2 and Smad3 in each group remained unchanged. These results indicate that overexpression of TREM2 weakens the phosphorylation of Smad2/3 induced by TGF-β, thereby inhibiting the downstream activation of EMT. Conversely, knockdown of TREM2 enhances the phosphorylation of Smad2/3 and promotes the progression of EMT, further demonstrating the role of TREM2 in inhibiting the TGF-β/Smad2/3/EMT axis.

TGF-β pathway activators can significantly promote the proliferation and migration of TREM2-overexpressing CCA cells

In order to further verify whether TREM2 affects the biological function of CCA cells through the TGF-β pathway, the TGF-β pathway activator (SRI-011381) was used to treat the stably transfected cells overexpressing TREM2 (Hucct1 cells), and the TGF-β pathway activator was used to promote the activation of the TGF-β pathway in the cells (Figure S2A). The effects on biological functions were observed by CCK-8 (Figure S2B), wound healing (Figure S2C), and Transwell migration experiments (Figure S2D). We observed that TGF-β pathway activators can reverse the reduction in cell proliferation and migration capacity caused by TREM2 expression upregulation. The above results show that TREM2 gene inhibits the proliferation and migration of CCA mainly by regulating the TGF-β pathway.

TREM2 promotes gemcitabine-induced apoptosis

We analyzed the effect of Hucct1 cells and RBE cells overexpressing TREM2 on the half-maximal inhibitory concentration (IC50) of gemcitabine by CCK-8 assay. TREM2 overexpression significantly reduced the gemcitabine IC50 in Hucct1 and RBE cells (**Figure 6A**), suggesting an increased sensitivity to gemcitabine. These data suggest that TREM2 status affects the chemotherapy resistance of CCA cells. In addition, we also used the TUNEL assay to analyze cell apoptosis. TUNEL assay showed that after gemcitabine treatment, the proportions of apoptotic and necrotic cells in the TREM2 overexpression group increased significantly (**Figure 6B**). Apoptosis and necrotic cells were significantly reduced in TREM2 knockdown cells. The above experimental results confirmed that TREM2 can promote gemcitabine-induced apoptosis of CCA cells.

Overexpression of TREM2 inhibited the growth of subcutaneous tumor in nude mice

The survival status and development of subcutaneous tumors in nude mice were monitored regularly following the subcutaneous injection of inoculated cells. On the 31st day after inoculation, the subcutaneous tumor diameter of nude mice was about 17 mm, and the mice were euthanized via cervical dislocation. The change of tumor growth volume with time was analyzed by two-way repeated measures analysis of variance and Sidak's multiple comparison test. Results showed that compared with the Hucct1-OENC group, both the subcutaneous tumor volume and weight in the Hucct1-OE group were significantly smaller than those in the control group (Hucct1-OENC group), with statistically significant differences, as shown in **Figure 7A**.

Using Western blot analysis, the expression levels of TREM2 and EMT-related markers were assessed in transplanted tumor tissues from nude mice. Results revealed that TREM2 and the epithelial marker E-cadherin were upregulated in the OE group compared to the NC group, while mesenchymal markers Vimentin, N-cadherin, and Slug were significantly decreased. These findings suggest that in vivo overexpression of TREM2 suppresses EMT marker expression and which may contribute to inhibited tumor progression (**Figure 7B**).

Discussion

TREM2, a transmembrane receptor of the immunoglobulin superfamily, is widely expressed on the surface of cells within the monocyte-

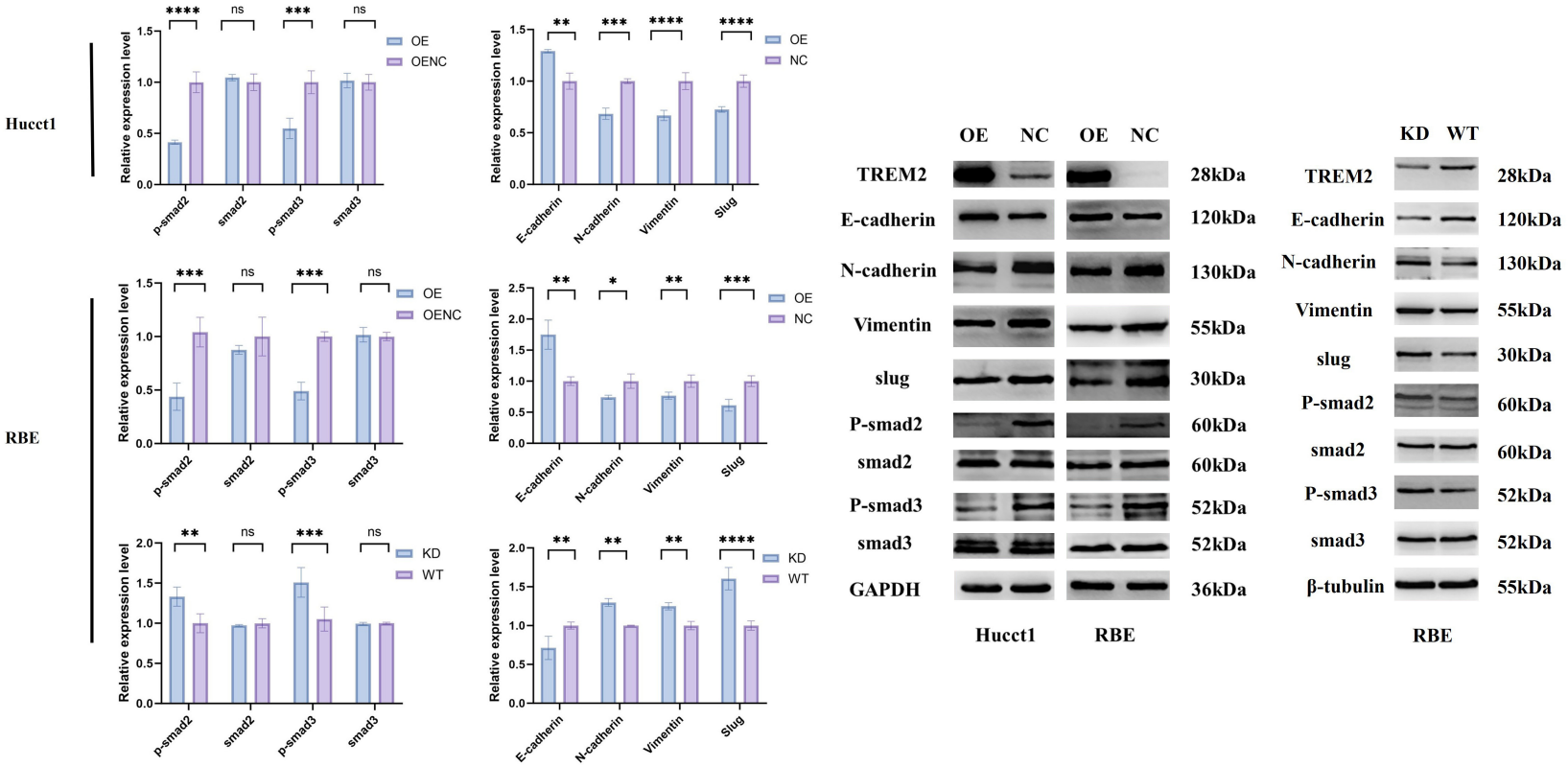

Figure 5. TREM2 regulates the occurrence of epithelial-mesenchymal transition in cholangiocarcinoma through the TGF-β/Smad2/3 signaling pathway. In CCA cells, overexpression of the TREM2 gene inhibited EMT via the TGF-β/Smad pathway: Western blot detection of p-Smad2, p-Smad3, Smad2, Smad3, E-cadherin, N-cadherin, Vimentin, Slug, expression in Hucct1 and RBE cells. $P < 0.05$ for OE group compared to OENC. Conversely, in the KD group, TREM2 knockdown promotes EMT by activating the TGF-β/Smad pathway.

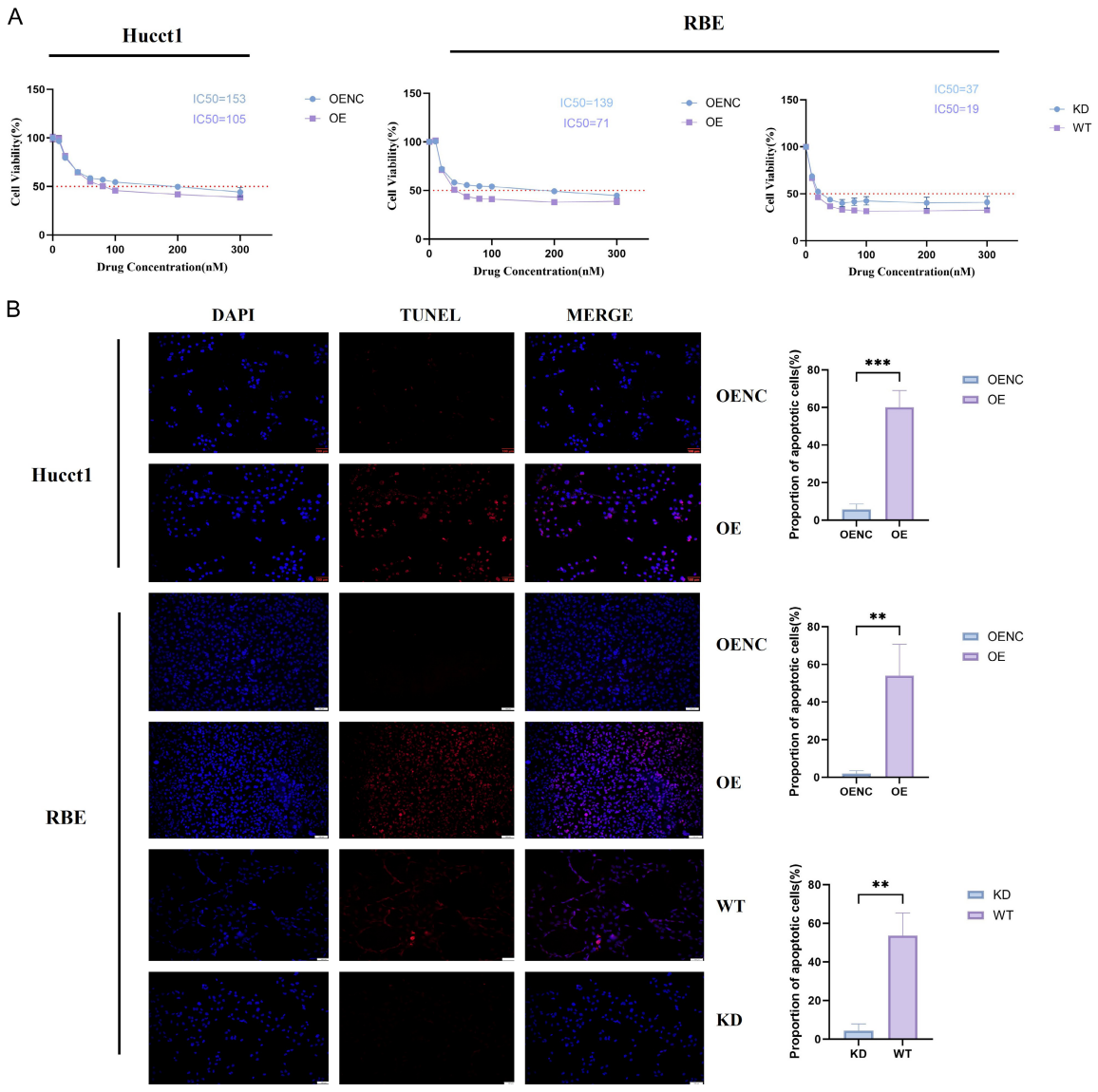

Figure 6. TREM2 promotes gemcitabine-induced apoptosis. A. In Hucct1 and RBE cells, the IC50 changes in the OE group and OENC group after gemcitabine treatment were detected and analyzed using the CCK-8 assay. The results showed that TREM2 overexpression significantly reduced the IC50 value of gemcitabine, while TREM2 downregulation significantly increased the IC50 value; B. TUNEL assay showed that after gemcitabine treatment, the apoptotic and necrotic cells in the TREM2 overexpression group increased significantly, and the difference was statistically significant. In the KD group, apoptosis of CCA cells was significantly inhibited (With magnification of 10×).

macrophage lineage, and is considered a marker for TAMs [8]. Furthermore, TREM2 also plays a significant role within the TME, where it can assist the immune escape of tumor cells by negatively regulating the anti-tumor immune response [15]. In cancers such as non-small cell lung cancer (NSCLC) and urothelial carcinoma (UC), TREM2$^+$ TAMs are associated with an immunosuppressive phenotype, correlating with poor prognosis [16-18]. In contrast, the study by Zhu et al. found that high TREM2$^+$ TAMs infiltration in skin malignant melanoma (SKCM) tissue was associated with increased tumor-infiltrating immune cells and longer cumulative survival, indicating a protective role [19]. In addition to this, TREM2 is linked to phagocytosis in glioma TME and acts as a significant immunomodulator [20]. High infiltration of TREM2$^+$ monocytes reduces tumor burden by both enhancing phagocytosis and inhibiting the inflammatory response, ultimately leading to longer survival times [21, 22]. These findings align with and support the results of our study.

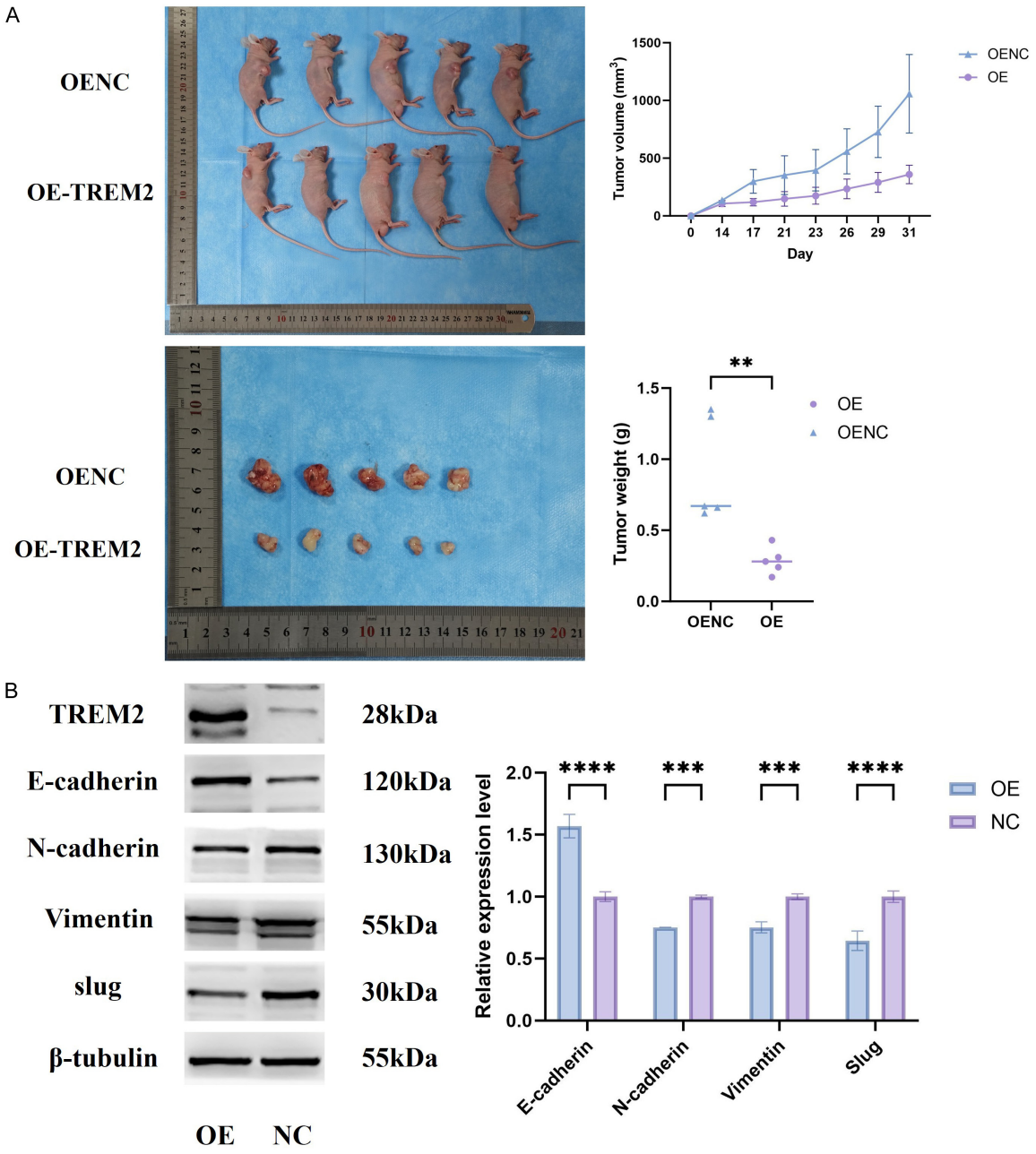

Figure 7. Overexpression of TREM2 inhibited the growth of subcutaneous tumor in nude mice. A. The comparison of tumor volume and weight in subcutaneous tumor-bearing nude mice following overexpression of TREM2 in Hucct1 cells demonstrated that both tumor volume and weight were lower in the OE-TREM2 group compared to the control (OENC) group; B. Up-regulation of TREM2 also inhibited the expression of EMT markers in vivo, thereby suppressing tumor formation: Western blot detected the expression of E-cadherin, N-cadherin, Vimentin, and Slug in the OE and NC groups.

In contrast to the well-defined role of TREM2 in immune cells, its function and clinical significance in CCA remain unclear. Our study aimed to fill this research gap by systematically investigating the expression, clinical relevance, and biological functions of TREM2 in CCA. Unlike findings reported in non-small cell lung cancer [16] or urothelial carcinoma [18], we observed high levels of TREM2 expression in the tumor stroma and tumor cells of CCA samples, which was associated with favorable clinicopathological features and a longer disease-free survival period. This finding is consistent with the tumor suppressive effect observed in colorectal cancer [13] and hepatocellular carcinoma [14].

Therefore, we speculate that in CCA, the high expression of TREM2 may also have the effect of inhibiting tumorigenesis and is related to the longer survival of patients. It is worth noting that although the overall level of TREM2 in tumor tissues is high, its expression will gradually decrease with the progress of staging. Furthermore, our research findings indicate that TREM2 is positively expressed on TAMs. Therefore, this dynamic change may be related to alterations in the tumor immune microenvironment, and the specific mechanism remains to be further explored. Moreover, multivariate logistic regression analysis confirmed that low levels of TREM2 protein expression were associated with tumor recurrence and metastasis, identifying it as an independent prognostic factor for CCA. The Kaplan-Meier (KM) curve analysis indicated that higher levels of TREM2 gene expression were associated with longer disease-free survival in CCA patients. In conclusion, TREM2 plays a critical role in regulating tumor development. The regulatory mechanisms of TREM2 vary across different cancers, necessitating a more comprehensive understanding of its regulatory roles within the tumor microenvironment.

Previous studies have shown that TREM2 is also widely expressed on tumor cells, and can modulate their proliferation and metastatic potential via a constellation of signaling pathways, ultimately influencing the advancement of tumorigenesis [9]. Upregulated expression of TREM2 was observed in tumor tissues from patients with gastric cancer (GC) [10], lung cancer [23], renal cell carcinoma (RCC) [24], and prostate cancer (PRAD) [25]. Furthermore, elevated TREM2 expression was significantly correlated with tumor stage and aggressive pathological features. TREM2 acts as an oncogene in tumor progression. In contrast, TREM2 acts as a tumor suppressor in CRC tissues. Overexpression of TREM2 can inhibit the progression of CRC by negatively regulating the Wnt/ERK/GSK-3β signaling pathway [13, 26, 27]. In acute myeloid leukemia (AML) [28], TREM2, a newly identified receptor for IL-34, induces bone marrow differentiation, thereby suppressing AML progression, through inhibition of the ERK1/2/Rasal3 signaling pathway. In the study by Tang W et al. [14], TREM2 also exhibited a tumor-suppressive effect. Overexpressed TREM2 inhibits the process of EMT in HCC cells by targeting and inhibiting the PI3K/Akt/β-Catenin pathway, which in turn inhibited the invasion and metastasis of HCC tumor cells. These suggest that TREM2 can inhibit tumor occurrence and development by activating different signaling pathways and plays an important role in tumor suppression. This dual functionality highlights the complexity of TREM2's mechanisms of action, whose functions appear to be tightly regulated by tumor type and cellular environment.

Crucially, our in vitro and in vivo functional studies clearly demonstrate that TREM2 functions as a tumor suppressor gene in cholangiocarcinoma. In this study, we found that TREM2 was also positively expressed on tumor cells of patients by double immunofluorescence. Moreover, in vitro functional experiments, we verified the effect of TREM2 on CCA cell biology through CCK-8 assays, plate cloning experiments and wound healing assay. The results showed that overexpression of TREM2 gene could inhibit the growth, proliferation, migration and invasion of CCA cells. These findings suggest that the TREM2 gene may be a tumor suppressor gene and play a role in inhibiting the growth, proliferation, migration and invasion of CCA cells.

Mechanistically, unlike the signaling pathways previously reported in colorectal cancer (CRC) (Wnt/ERK/GSK-3β) or hepatocellular carcinoma (HCC) (PI3K/Akt/β-Catenin), our functional study in CCA cells revealed a new signaling pathway axis. TREM2 can exert its tumor suppressor function through this signaling pathway axis. We demonstrated that overexpression of TREM2 would downregulate the TGF-β/Smad2/3 signaling pathway, resulting in inhibition of Smad2/3 phosphorylation, inhibition of EMT, and subsequent suppression of cell proliferation, migration, and invasion abilities. This effect is reversible after TGF-β stimulation, thereby confirming the causal relationship of this pathway. This identified the TGF-β/Smad2/3-EMT axis as the main mechanism by which TREM2 inhibits CCA. This finding has not been reported in other cancer types.

In addition to the role of TREM2 in the development of CCA itself, TREM2 also significantly affects the therapeutic response. Unlike previous studies that mainly focused on its immunological or intrinsic growth regulatory functions, we found that overexpression of TREM2 can enhance the chemosensitivity of CCA cells to gemcitabine, mainly through reducing its IC50 value and enhancing apoptosis. In contrast, knocking down TREM2 shows an opposite pattern. These results suggest that TREM2 status

may be relevant for chemotherapy sensitivity, potentially through EMT-associated drug tolerance programs and/or additional apoptosis-related mechanisms [29]. Further studies are warranted to delineate the downstream effectors linking TREM2 to chemotherapy response and to test whether TREM2 can improve predictive stratification in clinically treated cohorts.

Conclusions

In summary, this study elucidates a tumor-suppressive role for TREM2 in CCA, contrasting with its pro-tumorigenic functions in several other malignancies. Our study showed that in CCA tissues, the infiltration level of TREM2 positive cells in the tumor stroma and tumor cells was positively correlated with earlier clinical stage and longer disease-free survival of patients. In addition, TREM2 can also inhibit the EMT process by inhibiting the TGF-β/Smad2/3 signaling pathway, thereby affecting the proliferation and migration of CCA cells. It plays an important role in the occurrence and development of tumors and chemotherapy drug resistance. This finding provides an experimental basis for TREM2 as a potential tumor suppressor gene, and provides a theoretical basis for TREM2 as a prognostic marker and therapeutic target, which has important clinical translational potential.

Acknowledgements

This study was supported by the Natural Science Foundation of Gansu Province (23JRRA0986); The Program of Gansu Youth Science and Technology (20JR10RA755); Gansu Province College Teachers' Innovation Fund Program (2025B-019); Healthcare Industry Research Projects of Gansu Province (GSWSQN-2024-14).

Disclosure of conflict of interest

None.

Address correspondence to: Xiaojun Huang and Jinyong Hao, Department of Gastroenterology, The Lanzhou University Second Hospital, No. 82 Cuiyingmen, Linxia Road, Chengguan District, Lanzhou 730000, Gansu, China. Tel: +86-13919356123; ORCID: 0000-0002-1196-9381; E-mail: huangxj@lzu.edu.cn (XJH); Tel: +86-13679409066; ORCID: 0000-0001-8277-8294; E-mail: haojinyong517@sina.com (JYH)

References

[1] Vithayathil M and Khan SA. Current epidemiology of cholangiocarcinoma in Western countries. J Hepatol 2022; 77: 1690-1698.

[2] Vogel A, Bridgewater J, Edeline J, Kelley RK, Klümpen HJ, Malka D, Primrose JN, Rimassa L, Stenzinger A, Valle JW and Ducreux M; ESMO Guidelines Committee. Biliary tract cancer: ESMO Clinical Practice Guideline for diagnosis, treatment and follow-up. Ann Oncol 2023; 34: 127-140.

[3] Javle M, Lee S, Azad NS, Borad MJ, Kate Kelley R, Sivaraman S, Teschemaker A, Chopra I, Janjan N, Parasuraman S and Bekaii-Saab TS. Temporal changes in cholangiocarcinoma incidence and mortality in the United States from 2001 to 2017. Oncologist 2022; 27: 874-883.

[4] Liang HJ and Shen F. CSCO expert consensus on the diagnosis and treatment of biliary tract system tumors (2019 edition). J Clin Oncol 2019; 24: 828-838.

[5] Banales JM, Marin JJG, Lamarca A, Rodrigues PM, Khan SA, Roberts LR, Cardinale V, Carpino G, Andersen JB, Braconi C, Calvisi DF, Perugorria MJ, Fabris L, Boulter L, Macias RIR, Gaudio E, Alvaro D, Gradilone SA, Strazzabosco M, Marzioni M, Coulouarn C, Fouassier L, Raggi C, Invernizzi P, Mertens JC, Moncsek A, Ilyas SI, Heimbach J, Koerkamp BG, Bruix J, Forner A, Bridgewater J, Valle JW and Gores GJ. Cholangiocarcinoma 2020: the next horizon in mechanisms and management. Nat Rev Gastroenterol Hepatol 2020; 17: 557-588.

[6] Li RY, Qin Q, Yang HC, Wang YY, Mi YX, Yin YS, Wang M, Yu CJ and Tang Y. TREM2 in the pathogenesis of AD: a lipid metabolism regulator and potential metabolic therapeutic target. Mol Neurodegener 2022; 17: 40.

[7] Ulland TK, Song WM, Huang SC, Ulrich JD, Sergushichev A, Beatty WL, Loboda AA, Zhou Y, Cairns NJ, Kambal A, Loginicheva E, Gilfillan S, Cella M, Virgin HW, Unanue ER, Wang Y, Artyomov MN, Holtzman DM and Colonna M. TREM2 maintains microglial metabolic fitness in Alzheimer's disease. Cell 2017; 170: 649-663, e613.

[8] Molgora M, Liu YA, Colonna M and Cella M. TREM2: a new player in the tumor microenvironment. Semin Immunol 2023; 67: 101739.

[9] Khantakova D, Brioschi S and Molgora M. Exploring the impact of TREM2 in tumor-associated macrophages. Vaccines (Basel) 2022; 10: 943.

[10] Zhang X, Wang W, Li P, Wang X and Ni K. High TREM2 expression correlates with poor prognosis in gastric cancer. Hum Pathol 2018; 72: 91-99.

[11] Duggan SP, Garry C, Behan FM, Phipps S, Kudo H, Kirca M, Zaheer A, McGarrigle S, Reynolds

JV, Goldin R, Kalloger SE, Schaeffer DF, Long A, Strid J and Kelleher D. siRNA library screening identifies a druggable immune-signature driving esophageal adenocarcinoma cell growth. Cell Mol Gastroenterol Hepatol 2018; 5: 569-590.

[12] Zhang SL, Chen TS, Xiao L, Ye Y, Xia W and Zhang H. TREM2 siRNA inhibits cell proliferation of human liver cancer cell lines. Int J Clin Exp Pathol 2016; 9: 4318-4328.

[13] Kim SM, Kim EM, Ji KY, Lee HY, Yee SM, Woo SM, Yi JW, Yun CH, Choi H and Kang HS. TREM2 acts as a tumor suppressor in colorectal carcinoma through Wnt1/β-catenin and Erk signaling. Cancers (Basel) 2019; 11: 1315.

[14] Tang W, Lv B, Yang B, Chen Y, Yuan F, Ma L, Chen S, Zhang S and Xia J. TREM2 acts as a tumor suppressor in hepatocellular carcinoma by targeting the PI3K/Akt/β-catenin pathway. Oncogenesis 2019; 8: 9.

[15] Heinhuis KM, Ros W, Kok M, Steeghs N, Beijnen JH and Schellens JHM. Enhancing antitumor response by combining immune checkpoint inhibitors with chemotherapy in solid tumors. Ann Oncol 2019; 30: 219-235.

[16] Zhang H, Liu Z, Wen H, Guo Y, Xu F, Zhu Q, Yuan W, Luo R, Lu C, Liu R, Gu J and Ge D. Immunosuppressive TREM2(+) macrophages are associated with undesirable prognosis and responses to anti-PD-1 immunotherapy in non-small cell lung cancer. Cancer Immunol Immunother 2022; 71: 2511-2522.

[17] Molgora M, Esaulova E, Vermi W, Hou J, Chen Y, Luo J, Brioschi S, Bugatti M, Omodei AS, Ricci B, Fronick C, Panda SK, Takeuchi Y, Gubin MM, Faccio R, Cella M, Gilfillan S, Unanue ER, Artyomov MN, Schreiber RD and Colonna M. TREM2 modulation remodels the tumor myeloid landscape enhancing Anti-PD-1 immunotherapy. Cell 2020; 182: 886-900, e817.

[18] Song Y, Peng Y, Qin C, Wang Y, Yang W, Du Y and Xu T. Fibroblast growth factor receptor 3 mutation attenuates response to immune checkpoint blockade in metastatic urothelial carcinoma by driving immunosuppressive microenvironment. J Immunother Cancer 2023; 11: e006643.

[19] Zhu X, Zeng Z, Chen M, Chen X, Hu D, Jiang W, Du M, Chen T, Chen T, Liao W, Zhang C, Qu Y, Pan W and Zhong WI. TREM2 as a potential immune-related biomarker of prognosis in patients with skin cutaneous melanoma microenvironment. Dis Markers 2023; 2023: 8101837.

[20] Peshoff MM, Gupta P, Trivedi R, Oberai S, Chakrapani P, Dang M, Milam N, Maynard ME, Vaillant BD, Huse JT, Wang L, Clise-Dwyer K and Bhat KP. Triggering receptor expressed on myeloid cells 2 (TREM2) regulates phagocytosis in glioblastoma. bioRxiv 2023.

[21] Kluckova K, Kozak J, Szaboova K, Rychly B, Svajdler M, Suchankova M, Tibenska E, Filova B, Steno J, Matejcik V, Homolova M and Bucova M. TREM-1 and TREM-2 expression on blood monocytes could help predict survival in high-grade glioma patients. Mediators Inflamm 2020; 2020: 1798147.

[22] Kluckova K, Kozak J, Szaboova K, Suchankova M, Svajdler M, Blazickova S, Makohusova M, Steno J, Matejcik V and Bucova M. Low serum vitamin D levels are associated with a low percentage of TREM-2+ monocytes in low-grade gliomas and poorer overall survival in patients with high-grade gliomas. Bratisl Lek Listy 2021; 122: 172-178.

[23] Yao Y, Li H, Chen J, Xu W, Yang G, Bao Z, Xia D, Lu G, Hu S and Zhou J. TREM-2 serves as a negative immune regulator through Syk pathway in an IL-10 dependent manner in lung cancer. Oncotarget 2016; 7: 29620-34.

[24] Zhang H, Sheng L, Tao J, Chen R, Li Y, Sun Z and Qian W. Depletion of the triggering receptor expressed on myeloid cells 2 inhibits progression of renal cell carcinoma via regulating related protein expression and PTEN-PI3K/Akt pathway. Int J Oncol 2016; 49: 2498-2506.

[25] Gao HT, Yang Z, Sun H, Zhang Y, Wang Z, Liu WY, Wen HZ, Qu CB and Wang XL. TREM2 as an independent predictor of poor prognosis promotes the migration via the PI3K/AKT axis in prostate cancer. Am J Transl Res 2023; 15: 779-798.

[26] Taank Y and Agnihotri N. Understanding the regulation of β-catenin expression and activity in colorectal cancer carcinogenesis: beyond destruction complex. Clin Transl Oncol 2021; 23: 2448-2459.

[27] Qin CJ, Bu PL, Zhang Q, Chen JT, Li QY, Liu JT, Dong HC and Ren XQ. ZNF281 regulates cell proliferation, migration and invasion in colorectal cancer through Wnt/β-catenin signaling. Cell Physiol Biochem 2019; 52: 1503-1516.

[28] Xie X, Zhang W, Xiao M, Wei T, Qiu Y, Qiu J, Wang H, Qiu Z, Zhang S, Pan Y, Mao L, Li Y, Guo B, Yang W, Hu Y, Hu S, Gong Y, Yang J, Xiao G, Zhang Y and Bai X. TREM2 acts as a receptor for IL-34 to suppress acute myeloid leukemia in mice. Blood 2023; 141: 3184-3198.

[29] Zhang CX, Huang RY, Sheng G and Thiery JP. Epithelial-mesenchymal transition. Cell 2025; 188: 5436-5486.

Table S1. Baseline characteristics of CCA patients and the relationship between TREM2 expression levels and clinicopathologic features of CCA

Characteristic	n	Low expression	Medium expression	High expression	Pearson χ^2	*P*
TREM2	55	25 (45.5)	17 (30.9)	13 (23.6)		
Sex					1.707	0.426
Male	37	17 (45.9)	13 (35.1)	7 (18.9)		
Female	18	8 (44.4)	4 (22.2)	6 (33.3)		
Age					0.494	0.482
< 60	27	14 (51.9)	7 (25.9)	6 (22.2)		
≥ 60	28	11 (39.3)	10 (35.7)	7 (25)		
Position					0.034	0.983
Intrahepatic cholangiocarcinoma	35	16 (45.7)	11 (31.4)	8 (22.9)		
Hilar cholangiocarcinoma	20	9 (45.0)	6 (30.0)	5 (25.0)		
Differentiation					14.370	0.073
High	3	1 (33.3)	2 (66.7)	0 (0.0)		
High-middle	5	0 (0.0)	1 (20.0)	4 (80.0)		
Middle	24	13 (54.2)	8 (33.3)	3 (12.5)		
Moderate-poor	17	7 (41.2)	5 (29.4)	5 (29.4)		
Poor	6	4 (66.7)	1 (16.7)	1 (16.7)		
T					18.914	0.004
T1	10	0 (0.0)	6 (60.0)	4 (40.0)		
T2	26	11 (42.3)	7 (26.9)	8 (30.8)		
T3	5	2 (40.0)	2 (40.0)	1 (20.0)		
T4	14	12 (85.7)	2 (14.3)	0 (0.0)		
N					5.215	0.074
N0	37	13 (35.1)	13 (35.1)	11 (29.7)		
N1 and N2	18	12 (66.7)	4 (22.2)	2 (11.1)		
M					4.939	0.085
M0	52	22 (42.3)	17 (32.7)	13 (25)		
M1	3	3 (100.0)	0 (0.0)	0 (0.0)		
AJCC staging					14.353	0.026
IA-IB	9	0 (0.0)	5 (55.6)	4 (44.4)		
II	17	6 (35.3)	5 (29.4)	6 (35.3)		
IIIA-IIIC	25	16 (64.0)	6 (24.0)	3 (12.0)		
IVA-IVB	4	3 (75.0)	1 (25.0)	0 (0.0)		
Size					0.558	0.757
≤ 5	38	17 (44.7)	11 (28.9)	10 (26.3)		
> 5	17	8 (47.1)	6 (35.3)	3 (17.6)		
TBIL					0.005	0.946
< 26	33	14 (42.4)	12 (36.4)	7 (21.2)		
≥ 26	22	11 (50.0)	5 (22.7)	6 (27.3)		
γ-GT					1.059	0.586
≤ 60	17	6 (35.3)	6 (35.3)	5 (29.4)		
> 60	38	19 (50.0)	11 (28.9)	8 (21.1)		
ALP					0.209	0.901
≤ 125	15	7 (46.7)	4 (26.7)	4 (26.7)		
> 125	40	18 (45.0)	13 (32.5)	9 (22.5)		

AFP					0.579	0.749
≤ 7	48	21 (43.8)	15 (31.3)	12 (25.0)		
> 7	7	4 (57.1)	2 (28.6)	1 (14.3)		
CEA					4.823	0.090
≤ 3.4	34	15 (44.1)	18 (23.5)	11 (32.4)		
> 3.4	21	10 (47.6)	9 (42.9)	2 (9.5)		
CA125					0.004	0.998
≤ 35	42	19 (45.2)	13 (31.0)	10 (23.8)		
> 35	13	6 (46.2)	4 (30.8)	3 (23.1)		
CA199					1.925	0.382
≤ 27	17	6 (35.3)	5 (29.4)	6 (35.3)		
> 27	38	19 (50.0)	12 (31.6)	7 (18.4)		
Recurrence time					28.445	< 0.001
≤ 12	33	22 (66.7)	10 (30.3)	1 (3.0)		
> 12	15	3 (20.0)	5 (33.3)	7 (46.7)		
> 24	7	0 (0.0)	2 (28.6)	5 (71.4)		

Table S2. Univariate and multivariate analysis of 1-year recurrence rate in CCA patients

	Univariate analysis		Multivariate analysis	
	OR (95% CI)	P	OR (95% CI)	P
TREM2 expression				
Low	88 (8.227-941.327)	< 0.001	88.239 (5.609-1388.119)	0.001
Medium	17.143 (1.794-163.806)	0.014	22.000 (1.630-297.011)	0.020
High	Reference		Reference	
Sex				
Male	Reference			
Female	0.384 (0.121-1.221)	0.105		
Age				
< 60	Reference			
≥ 60	1.440 (0.487-4.255)	0.509		
Position				
Intrahepatic cholangiocarcinoma	Reference			
Hilar cholangiocarcinoma	0.722 (0.237-2.205)	0.568		
Differentiation				
High	2.000 (0.112-35.807)	0.638		
High-middle	0.250 (0.017-3.770)	0.317		
Middle	2.000 (0.327-12.238)	0.453		
Moderate-poor	1.833 (0.279-12.066)	0.528		
Poor	Reference			
T				
T1	Reference			
T2	6.400 (1.124-36.437)	0.036		
T3	2.667 (0.250-28.438)	0.417		
T4	52.000 (4.032-670.597)	0.002		
N				
N0	Reference			
N1 and N2	3.316 (0.918-11.981)	0.067		

AJCC staging				
IA-IB	Reference		Reference	
II	11.429 (1.155-113.115)	0.037	15.639 (0.803-304.626)	0.070
IIIA-IIIC	25.333 (2.611-245.815)	0.005	13.829 (0.798-239.731)	0.071
IVA-IVB	24.000 (1.111-518.518)	0.043	5.169 (0.147-181.980)	0.366
Size				
≤ 5	Reference			
> 5	2.925 (0.806-10.615)	0.103		
TBIL				
< 26	Reference			
≥ 26	0.939 (0.313-2.820)	0.911		
γ-GT				
≤ 60	Reference			
> 60	1.524 (0.479-4.852)	0.476		
ALP				
≤ 125	Reference			
> 125	0.676 (0.195-2.345)	0.538		
AFP				
≤ 7	Reference			
> 7	1.786 (0.314-10.147)	0.513		
CEA				
≤ 3.4	Reference		Reference	
> 3.4	4.781 (1.329-17.206)	0.017	5.740 (0.891-36.953)	0.066
CA125				
≤ 35	Reference			
> 35	2.754 (0.662-11.462)	0.164		
CA199				
≤ 27	Reference			
> 27	1.524 (0.479-4.852)	0.476		

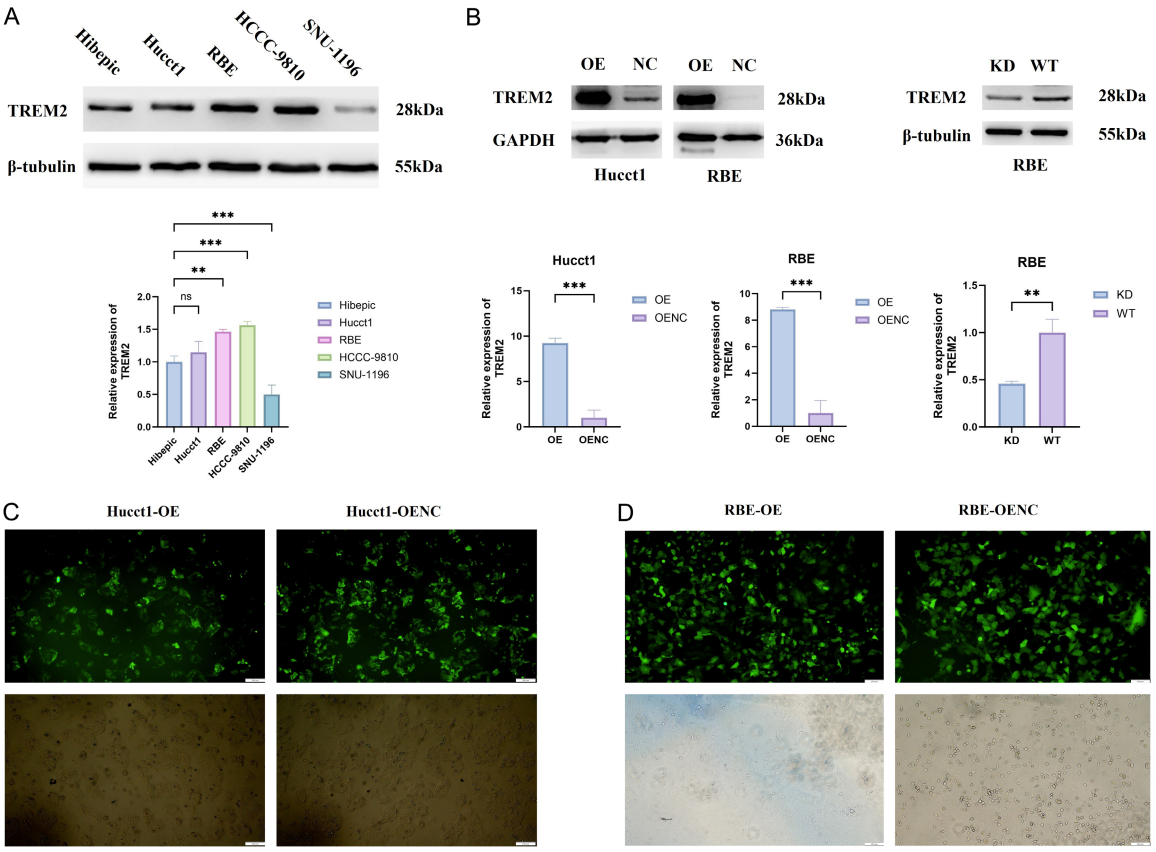

Figure S1. Differential expression of TREM2 in Hibepic and CCA cell lines and Validation of Protein Levels Following TREM2 Gene Upregulation/Downregulation. (A) TREM2 expression levels in different CCA cell lines: The expression levels of TREM2 in CCA cells (Hucct1, RBE, HCCC-9810, SNU-1196) and normal cell lines (Hibepic) were detected by Western blot; (B) The efficiency of overexpression and knockdown was verified by Western blot analysis, and the results showed that the TREM2 gene was significantly upregulated/downregulated in Hucct1 and RBE cells, $P < 0.05$; (C, D) The above Hucct1 cell line (C) and RBE cell line (D) were transfected with lentivirus (lentiviral vector carrying green fluorescent protein gene, GFP). The expression of GFP was observed under a fluorescence microscope within 1 week after transfection (With magnification of 10×). The intensity of green fluorescence expression was positively correlated with the number of virus particles infected by the target cells.

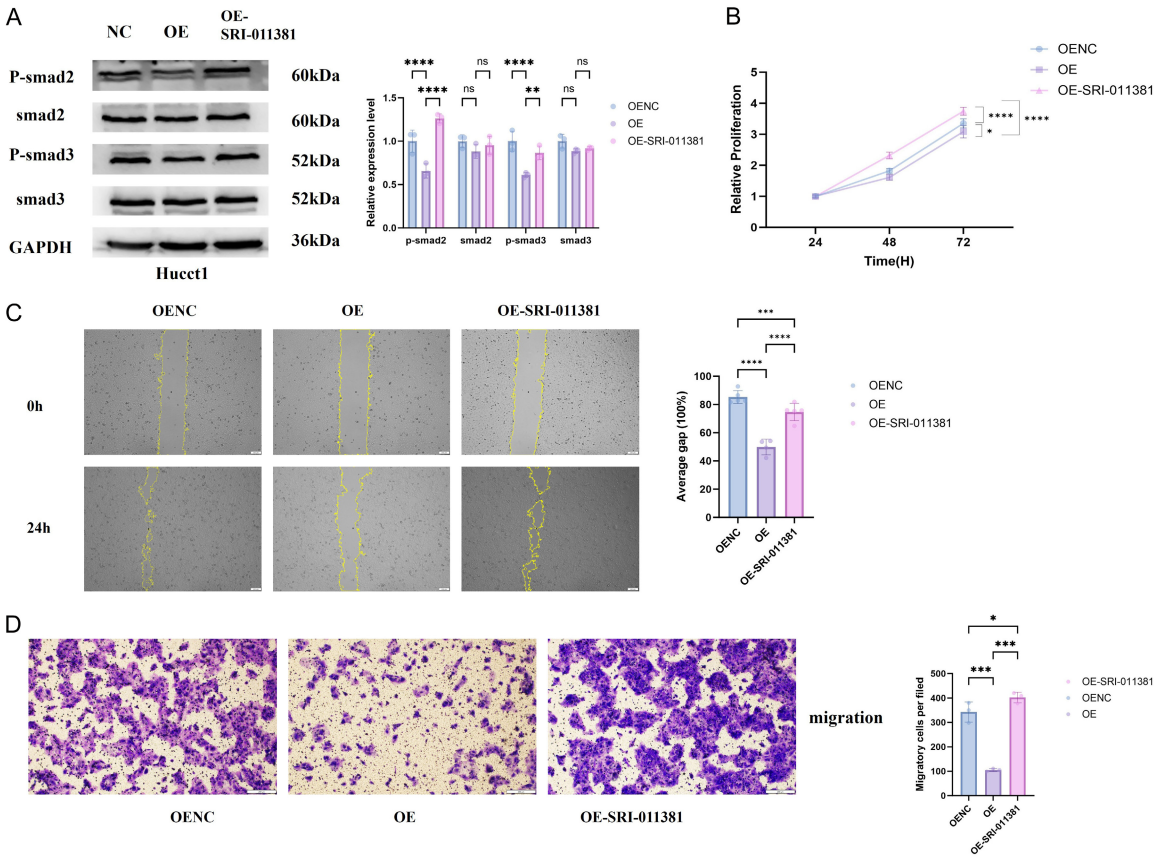

Figure S2. TGF-β pathway activators can significantly promote the proliferation and migration of TREM2-overexpressing CCA cells. A. Expression of the key molecule p-Smad2/3 in the TGF-β pathway after treatment of Hucct1 cells with the TGF-β activator SRI-011381 in the OE group and OENC group; B. CCK-8 assay results show that the TGF-β activator can reverse the decreased proliferation capacity caused by TREM2 overexpression; C. Cell wound healing assay results show that TGF-β activators can reverse the decrease in migration capacity caused by TREM2 overexpression (With magnification of 4×); D. Transwell migration assay results show that TGF-β activators can reverse the decrease in migration capacity caused by TREM2 overexpression (With magnification of 10×).